Supporting information for

AIEgen-Functionalized Metal-Organic Gel as Bifunctional Platform for Efficient Adsorption and Portable Sensing of Gaseous Iodine

Jian Xie,[a] Ji Lei,[a] Lilin Zhang,[b] Jinpeng Liang,[a] Sen Mei,[c] Lixi Chen,[c] Xia Wang,[b] Wei Liu,[b]

Yanlong Wang,[c] Baowei Hu[a*]*

[a] School of Life and Environmental Sciences, Shaoxing University, Shaoxing, 312000, China

[b]*School of Environmental and Material Engineering, Yantai University, Yantai 264005, China*

[c]*State Key Laboratory of Radiation Medicine and Protection, School of Radiological and Interdisciplinary Sciences (RAD-X), Collaborative Innovation Center of Radiation Medicine of Jiangsu Higher Education Institutions, Soochow University, Suzhou 215123, China*

Materials and reagents

1,1,2,2-tetra(4-carboxylphenyl)ethylene (95%), $Zr(NO_3)_4 \cdot 5H_2O$ (98%), iodine (99.8%), methane iodide (98 %) and Polyvinylpyrrolidone (PVP, Mw~1300000) were bought from Macklin Inc.; ethanol (99.5%), methanol (>99.5%) and *N,N*-dimethylformamide (DMF, 99.9%) were bought from Sinopharm Chemical Reagent Co., Ltd.

Experimental Section

Synthesis of YTU-G-1. All reagents and solvents were purchased from commercial suppliers and used as received without further purification. 1,1,2,2-tetra(4-carboxylphenyl)ethylene ($C_{30}H_{20}O_8$, 10 mg) and $Zr(NO_3)_4 \cdot 5H_2O$ (50 mg) were uniformly dispersed in the mixture of N,N'-dimethylformamide (DMF, 3 mL) and distilled water (3 mL) under ultrasonic treatment. The resulted sample was heated to 100 °C for 24 h. Finally, the solid samples were washed with distilled water at room temperature and dried through a freeze drier at -90 °C for 24 h.

Preparation of YTU-G-1@PVP Composite Membrane. The ET-1334 electrospinning apparatus was used to prepare the **YTU-G-1**@PVP nanofiber thin films. First, PVP was mixed with methanol at a weight ratio of 1 : 10, which was evenly mixed on a magnetic mixer. Then, fully ground **YTU-G-1** was added to the previous mixture, and stirred for 10 h. After that, pouring the evenly mixed solution into a 12 mm inner diameter jet pump. Finally, the flexible **MOG**@PVP composite membrane was obtained by electro-spinning.

Iodine detection and adsorption experiments. 200 mg Iodine was weighted and dissolved in 50 mL ethanol at room temperature (25 °C) to obtain an iodine solution (4 g/L). Various volumes of iodine solution (0, 12.5, 25, 50, 75, 125, 175 and 250 μL) and 20 mg of **YTU-G-1** powder (or 10×10 mm **MOG**@PVP membranes) were added into a reagent bottle (1 L). The reagent bottle was then heated at 75 °C for 5 min for powder samples (or 10 min for membrane samples) to generate iodine vapor with different concentration (0, 50, 100, 200, 300, 500, 700 and 1000 ppb). Then, samples were removed from reagent bottles and luminescence spectra were collected. Iodine

gas adsorption capability was evaluated through gravimetric analysis. Sample vials containing 20 mg of **YTU-G-1** and 300 mg of solid iodine were placed in sealed vials and stored at 75 °C to capture iodine. At the end of adsorption, the free iodine vapor is removed and the materials were weighed. Adsorption capacity was calculated according to the following formula:

$$Qt = (w_2-w_1)/w_1\times100\ wt\%$$

where w_1 and w_2 are the weights of **YTU-G-1** before and after iodine capture. After iodine absorption, **YTU-G-1** was desorbed at 120 °C. The mass loss of **YTU-G-1** saturated with adsorbed iodine was weighed at room temperature and ordinary pressure for 0, 12, 24, 48, 72, 96 h, and the adsorption stability of **YTU-G-1** was tested.

Materials and Instrumentation. The surface morphology of **YTU-G-1** was analyzed by scanning electron microscopy (SEM, FEI Quanta 200 FEG). The micromeritics ASAP 2020 surface aperture analyzer was used to record the N_2 adsorption-desorption isotherms of **YTU-G-1** at 77 K. Powder X-ray diffraction (PXRD) patterns of the **YTU-G-1** samples were measured by a Bruker D8-Venture single crystal X-ray diffractometer with Cu Kα radiation, and the scan rate is 10 °/min. The luminescence spectra of **YTU-G-1** before and after iodine loading were measured by integrating sphere and steady-state transient luminescence spectrometer (FLS980, λ_{ex} = 365 nm). Raman Microscopy (Labram HR800, an excitation wavelength of 532 nm) was adopted to analyze the nature of trapped iodine on the **YTU-G-1** samples. Furthermore, the iodine-loaded **YTU-G-1** was analyzed by X-ray photoelectron spectroscopy (XPS). The Fourier transform infrared spectra (FTIR, Aglient Cary 630) of **YTU-G-1** before and after iodine loading were measured with the KBr pressed-disk method. The hydrolytic stability of **YTU-G-1** was tested by inductively coupled plasma-mass spectrometry (Thermo Scientific iCAP RQ ICP-MS).

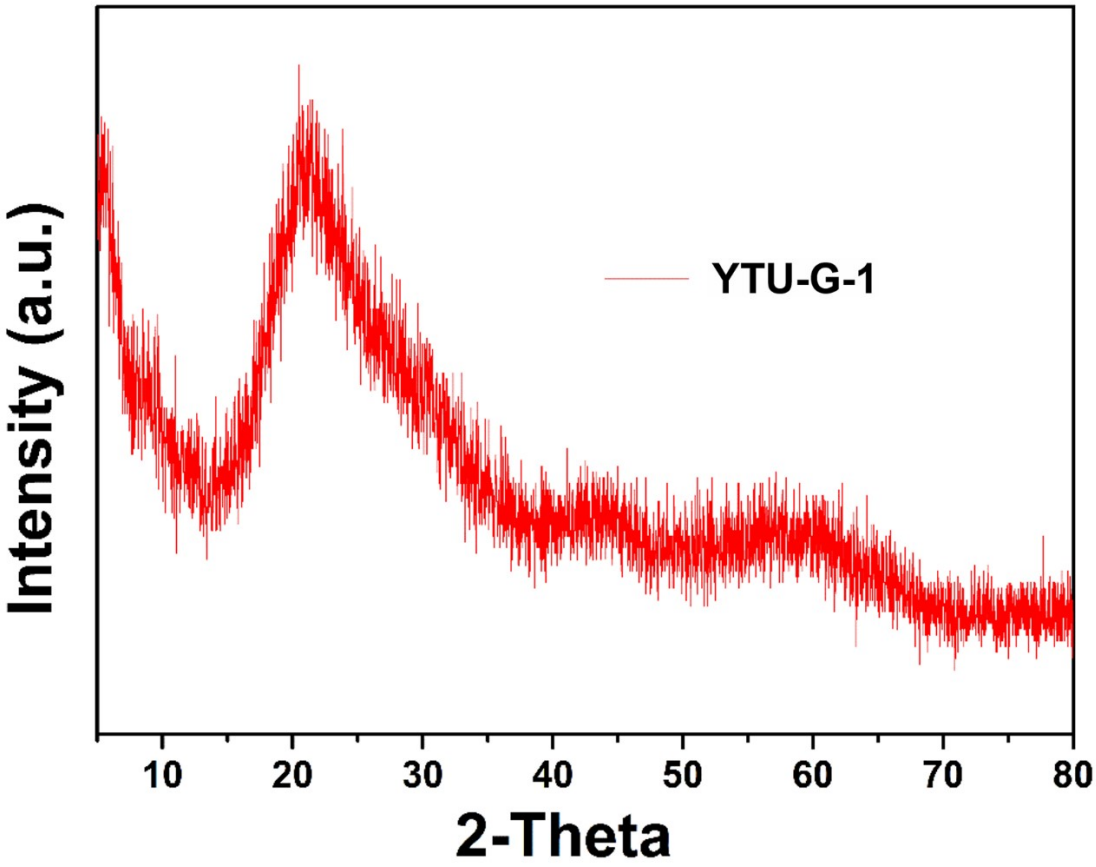

Fig. S1 PXRD pattern of **YTU-G-1**.

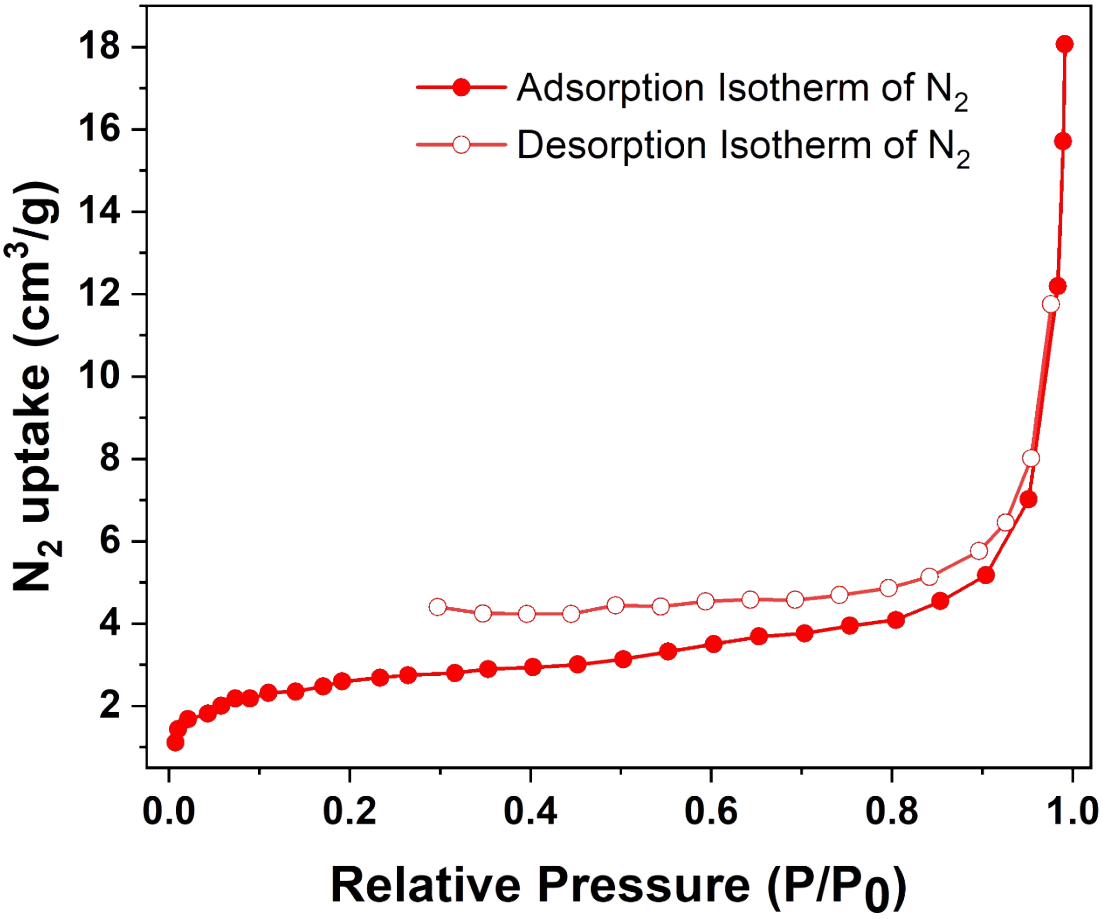

Fig. S2 N_2 adsorption and desorption isotherms for **YTU-G-1** at 77 K.

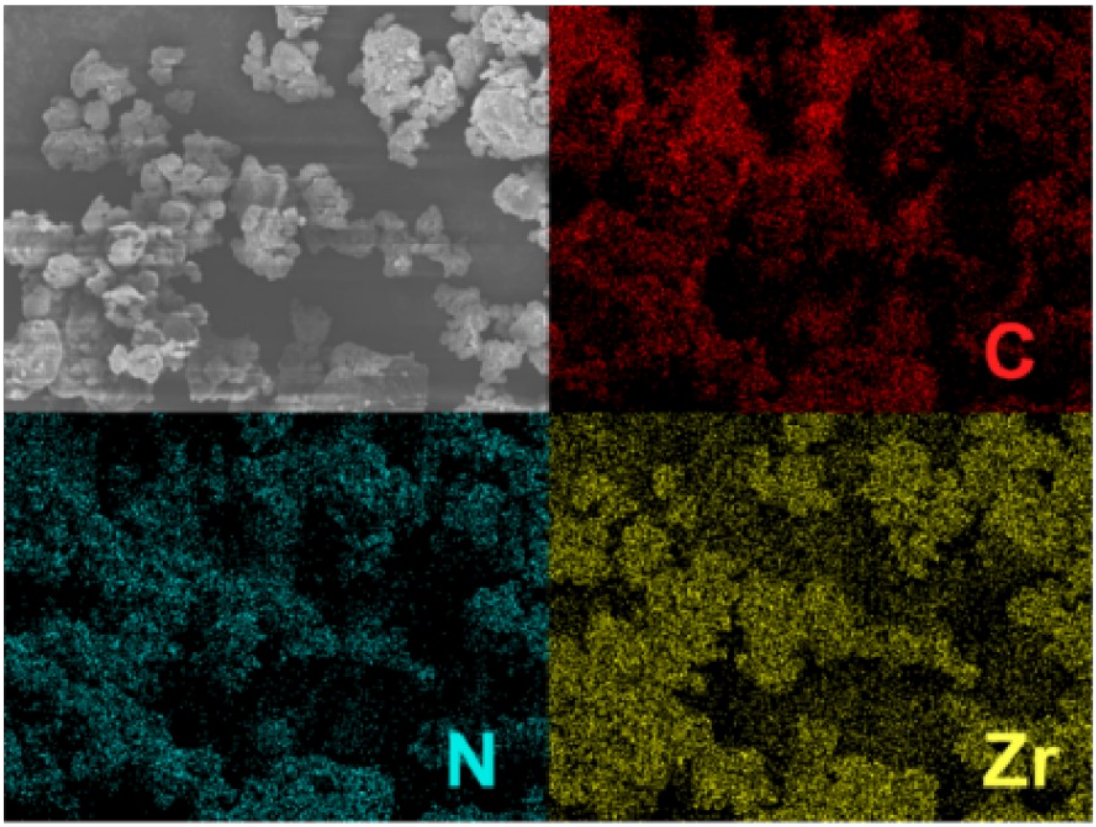

Fig. S3 SEM image of **YTU-G-1** and element-mapping images of C, N, Zr.

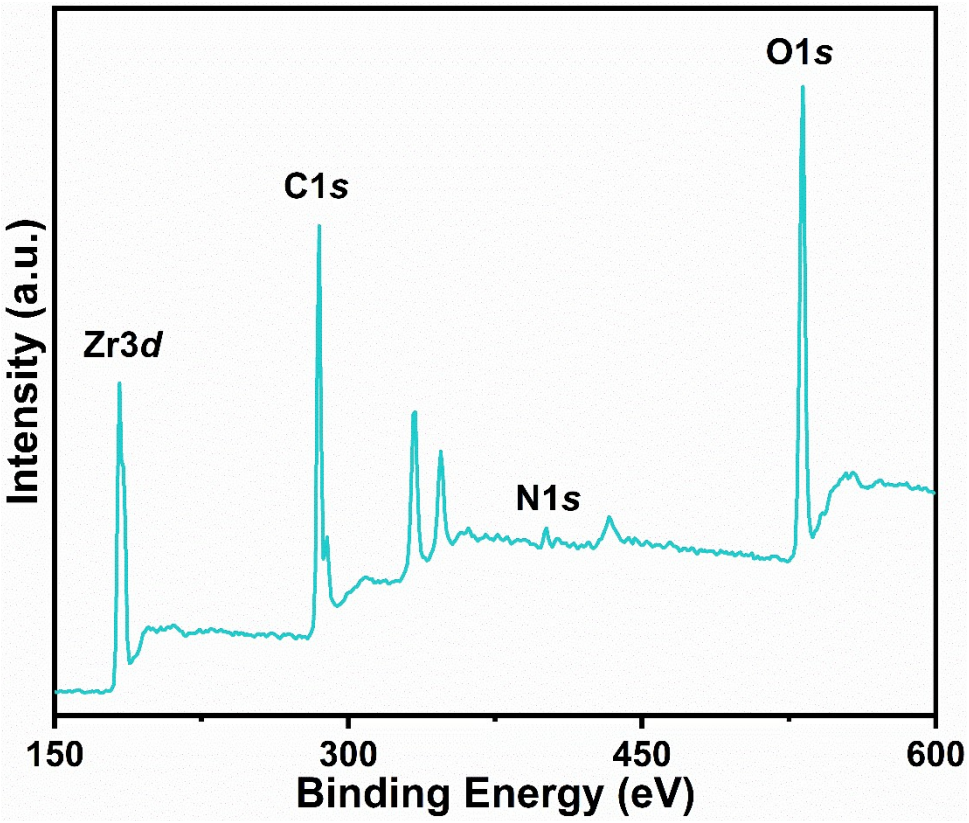

Fig. S4 XPS spectrum of **YTU-G-1**.

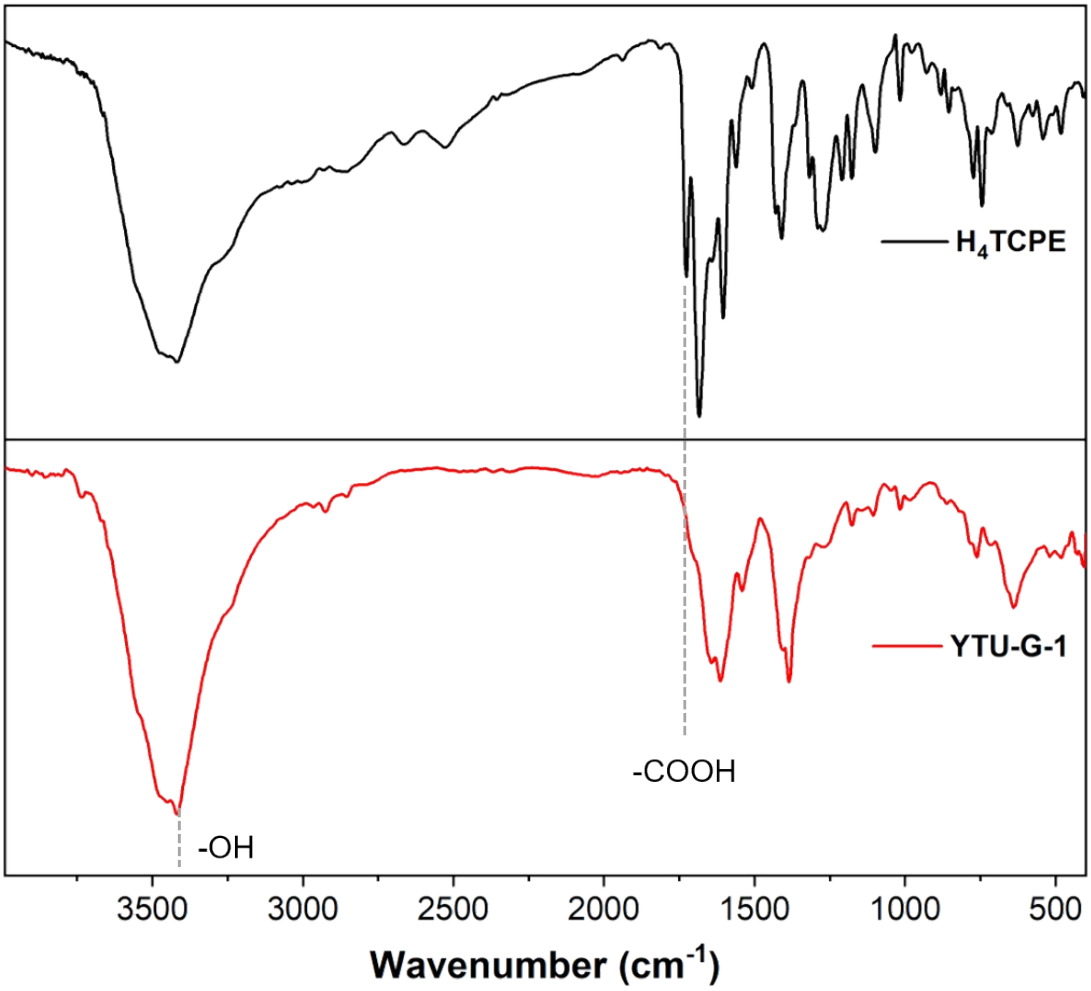

Fig. S5. FTIR spectra of H_4TCPE and **YTU-G-1**.

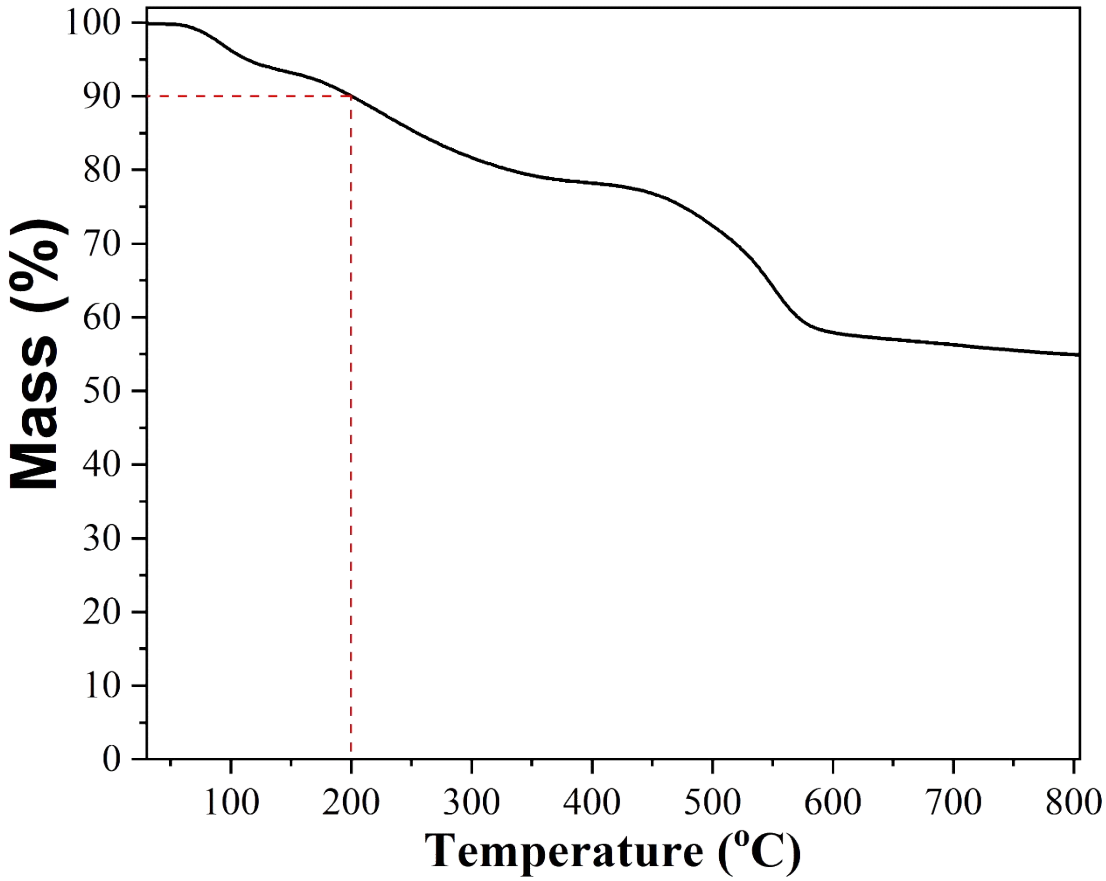

Fig. S6. TGA curve of **YTU-G-1.**

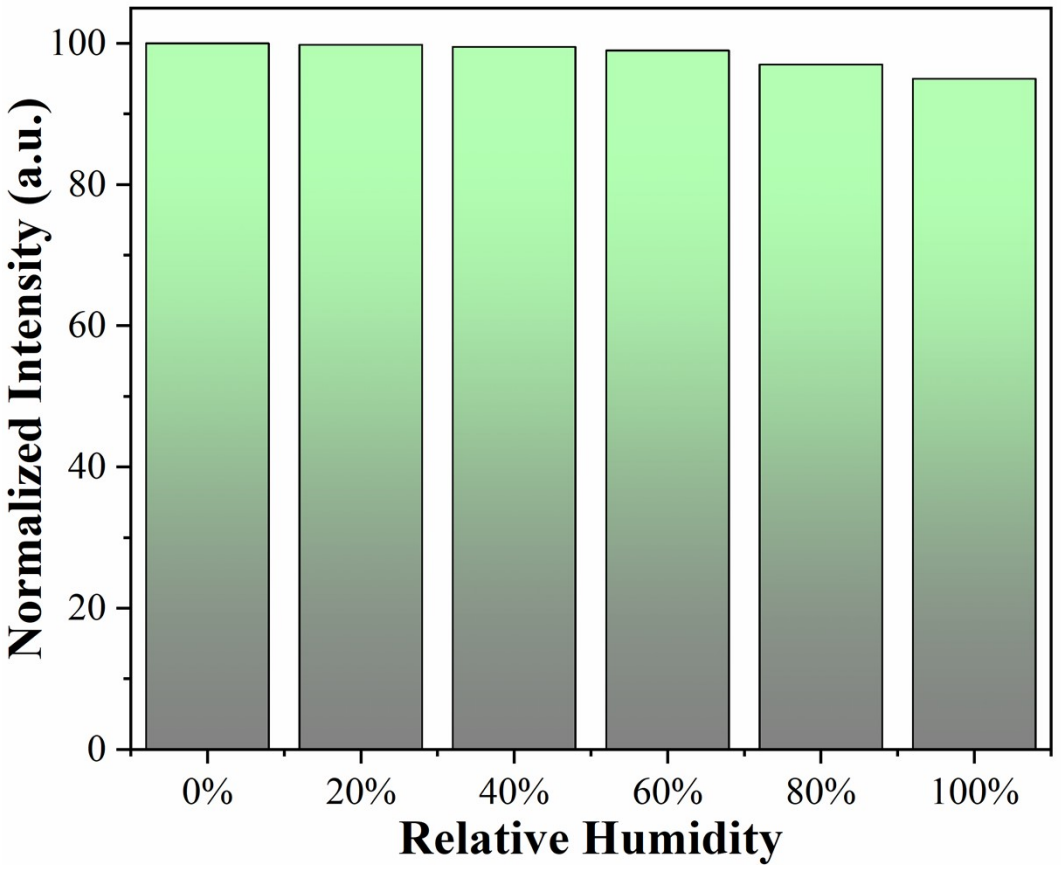

Fig. S7. The effect of humidity on the fluorescent properties of **YTU-G-1.**

Table S1. Summary of adsorption capacity of materials for iodine vapor capture

Sample	Category	Adsorption capacity（g/g）	Ref.
BN-Cu	aerogels	17.4	J. Hazard. Mater. 2023, 460, 132481.
BN-Ag	aerogels	22.3	J. Hazard. Mater. 2023, 460, 132481.
Bi@SNF	aerogels	0.98	Langmuir 2023, 39, 12910–1291.
polymerP1	pyridine gels	2.49	Polym. Chem. 2023, 14, 4109–4115.
polymerP2	pyridine gels	2.581	Polym. Chem. 2023, 14, 4109–4115.
polymerP3	pyridine gels	2.99	Polym. Chem. 2023, 14, 4109–4115.
COFA-1	aerogels	8.15	Chem. Mater. 2022, 34, 11062–11071.
COFP-1	aerogels	5.84	Chem. Mater. 2022, 34, 11062–11071.
COFA-2	aerogels	5.16	Chem. Mater. 2022, 34, 11062–11071.
COFA-3	aerogels	6.58	Chem. Mater. 2022, 34, 11062–11071.
G-TP5	organogels	0.67	Angew. Chem. Int. Ed. 2019, 58, 3885–3889.
G-TP6	organogels	0.58	Angew. Chem. Int. Ed. 2019, 58, 3885–3889.
G-QP5	organogels	0.35	Angew. Chem. Int. Ed. 2019, 58, 3885–3889.
G-QP6	organogels	0.49	Angew. Chem. Int. Ed. 2019, 58, 3885–3889.
Zr@MG	xerogels	2.32	J. Colloid Interf. Sci. 2023, 633, 441–452.
AgI-HTX-150	xerogels	0.429	ACS Omega 2021, 6, 11628–11638.
HAP@Ge(0.2/1)	cryogels	2.242	Collagen and Leather 2023, 5, 32.
HAP@Ge(0.5/1)	cryogels	2.693	Collagen and Leather 2023, 5, 32.
HAP@Ge(1/1)	cryogels	1.837	Collagen and Leather 2023, 5, 32.
CuOx/Al2O3	aerogels	0.347	J. Hazard. Mater. 2023, 443, 130349.
Mg@TAEA	metallohydrogels	0.513	Langmuir 2022, 38, 10601–10610.
Ag0-Aerogel	aerogels	0.375	Microporous Mesoporous Mater. 2022, 336, 111898.
CWNU	MOGs	3.36	Inorg. Chem. 2022, 61, 4818–4824.
CWNU-NH	MOGs	4.1	Inorg. Chem. 2022, 61, 4818–4824.
CWNU-2NH2	MOGs	4.2	Inorg. Chem. 2022, 61, 4818–4824.
TPMB-tube-P5	Supramolecular gels	2.29	Colloids Surf. A: Physicochem. Eng. Aspects 2021, 628, 127347.
PEIXG	xerogels	1.88	ACS Appl. Polym. Mater. 2020, 2, 152–158.
CoFe@CA-IS	aerogels	0.194	Microporous Mesoporous Mater. 2020, 306, 110386
CoFe@CA-D	aerogels	0.457	Microporous Mesoporous Mater. 2020, 306, 110386
BisImi-POP@2	POPs	10.30	Polym. Mater. 2021, 3, 1, 354–361.
iCOF-AB-33	CPFs	9	Angew. Chem. Int. Ed. 2021, 60, 22432–22440.
iPOP	POPs	7.3	ACS Appl. Mater. Interfaces 2021, 13, 34188−34196.
SR-KOH	PCs	6.46	Chem. Eng. J. 2019, 372, 65−73.
T-Hex	HOFs	6.4	Adv. Funct. Mater. 2024, 34, 2311964.
USTB-1c	POCs	5.8	J. Am. Chem. Soc. 2022, 144, 12390−12399.
BPPOC	POCs	5.64	J. Am. Chem. Soc. 2022, 144, 12390−12399.
OMC3	POCs	3.78	Angew. Chem. Int. Ed. 2020, 59, 20846–20851.
Bpy-Cage	POCs	3.21	Chem. Eur. J. 2016, 22, 11863–11868.
BTPOC	POCs	3.21	Chem. Eng. J. 2022, 428, 131129.
HCOF-1	HOFs	2.9	J. Am. Chem. Soc. 2017, 139, 7172−7175.
OMC-1	OMCs	2.25	Chem. Asian J. 2021, 16, 142–146.
OMC-2	OMCs	2.15	Chem. Asian J. 2021, 16, 142–146.
B-Hex	OMCs	0.92	Adv. Funct. Mater. 2024, 34, 2311964.
AlOC-26-NC	OMCs	0.7	J. Am. Chem. Soc. 2021, 143, 2325−2330.
HISL	Inorganic materials	0.53	J. Am. Chem. Soc. 2010, 132, 8897–8899.
SL-1	Inorganic materials	0.48	J. Am. Chem. Soc. 2010, 132, 8897–8899.
Si-BEA	Inorganic materials	0.47	J. Am. Chem. Soc. 2010, 132, 8897–8899.
AC	Inorganic materials	0.7	J. Am. Chem. Soc. 2010, 132, 8897–8899.
C@ETS-10	Inorganic materials	0.04	Chem. Eng. J. 2016, 287, 593–601.
MIL-101-Cr-HMTA	MOFs	0.83	Nat. Commun. 2022, 13, 2878.
SCU-COF-2	COFs	6	Chem, 2021, 7, 699−714.
iCOF-AB-50	COFs	2.79	Angew. Chem. Int. Ed. 2021, 60, 22432–22440.
TGDM	COFs	0.3	J. Am. Chem. Soc. 2022, 144, 6821−6829.
JUC-561	COFs	0.2	J. Am. Chem. Soc. 2022, 144, 6821−6829.
COF-TAPT	COFs	1.25	Nat. Commun. 2022, 13, 2878.
COF-TAPB	COFs	1.12	Nat. Commun. 2022, 13, 2878.

TFPA-TAPT	COFs	0.42	Nat. Commun. 2022, 13, 2878.
$[Cd(L^1)_2](ClO_4)_2$[a]	MOFs	0.46	Chem. Commun. 2011, 47, 7185–7187.
$[Cd_3(BTC)_2(TIB)_2]$[a]	MOFs	0.03	J. Solid State Chem. 2015, 223, 23–31.
$[Zn_3(BTC)_2(TIB)_2]$[a]	MOFs	0.04	J. Solid State Chem. 2015, 223, 23–31.
$[Cu_2(bitmb)_2Cl_4]$[a]	MOFs	0.31	J. Am. Chem. Soc. 2006, 128, 698–699.
Cu-BTC	MOFs	1.75	Chem. Mater. 2013, 25, 2591−2596.
$[Cu_4I_4(L^3)]$	MOFs	0.14	Chem. Commun. 2016, 52, 12702−12705.
$[Fe_3(HCOO)_6]$	MOFs	0.49	Adv. Funct. Mater. 2007, 17, 1523–1536.
MIL-53-SH(Al)	MOFs	0.33	Cryst. Eng. Comm. 2016, 18, 8108–8114.
Ca(sdb)	MOFs	0.26	ACS Appl. Mater. Interfaces 2018, 10, 10622−10626.
Ca(tcpb)	MOFs	0.43	ACS Appl. Mater. Interfaces 2018, 10, 10622−10626.
TMBP·CuI	MOFs	0.64	Inorg. Chem. 2014, 53, 6837−6843.
ZIF-8	MOFs	1.25	Cryst. Eng. Comm, 2014, 16, 8660–8663.
$[Zn_3(DL\text{-}lac)_2(pybz)_2]$	MOFs	1.01	J. Am. Chem. Soc. 2010, 132, 2561–2563.
$[Zn_2(\mu_4\text{-}ao_2btc)(\mu\text{-}pbix)_2]$	MOFs	0.2	Inorg. Chem. 2015, 54, 11283−11291.
Zn2(tptc)(apy)	MOFs	2.16	Inorg. Chem. 2016, 55, 9270−9275.
$[Zr_6O_4(OH)_4(L^4)_6]$	MOFs	1.07	Chem. Eur. J. 2016, 22, 4870–4877.
$[Zr_6O_4(OH)_4(L^5)_6]$	MOFs	1.8	Chem. Eur. J. 2016, 22, 4870–4877.
$[Zr_6O_4(OH)_4(L^6)_6]$	MOFs	1.8	Chem. Eur. J. 2016, 22, 4870–4877.
$[Zr_6O4(OH)_4(L^7)_6]$	MOFs	2.79	Chem. Eur. J. 2016, 22, 4870–4877
MFM-300(Sc)	MOFs	1.54	J. Am. Chem. Soc. 2017, 139, 16289–16296.
MFM-300(In)	MOFs	1.16	J. Am. Chem. Soc. 2017, 139, 16289–16296.
MFM-300(Fe)	MOFs	1.29	J. Am. Chem. Soc. 2017, 139, 16289–16296.
MFM-300(Al)	MOFs	0.94	J. Am. Chem. Soc. 2017, 139, 16289–16296.
MFM-300(V^{III})[a]	MOFs	1.42	Inorg. Chem. 2019, 58, 14145–14150.
MFM-300(V^{IV})[a]	MOFs	1.25	Inorg. Chem. 2019, 58, 14145–14150.
UPC-158	MOFs	1.78	J. Mater. Chem. A 2019, 7, 13173–13179.
UPC-158-HF	MOFs	2.19	J. Mater. Chem. A 2019, 7, 13173–13179.
UPC-158-HCl	MOFs	2.92	J. Mater. Chem. A 2019, 7, 13173–13179.
UPC-158-HBr	MOFs	2.75	J. Mater. Chem. A 2019, 7, 13173–13179.
UPC-158-HCl	MOFs	2.59	J. Mater. Chem. A 2019, 7, 13173–13179.
SION-8[a]	MOFs	0.25	Chem. Eur. J. 2019, 25, 501–506.
MOF-808	MOFs	2.18	ACS Appl. Mater. Interfaces 2020, 12, 20429–20439.
NU-1000	MOFs	1.45	ACS Appl. Mater. Interfaces 2020, 12, 20429–20439.
MOF-867	MOFs	0.88	ACS Appl. Mater. Interfaces 2020, 12, 20429–20439.
UiO-66	MOFs	1.17	Chemistry 2021, 3, 525–531.
UiO-66-FA	MOFs	2.25	Chemistry 2021, 3, 525–531.
UiO-67	MOFs	0.53	ACS Appl. Mater. Interfaces 2020, 12, 20429–20439.
PCN-333(Al)	MOFs	4.42	J. Mater. Chem. A 2019, 7, 18324–18329.
IL@PCN-333(Al)[b]	MOFs	7.35	J. Mater. Chem. A 2019, 7, 18324–18329.
YTU-G-1	MOGs	1.398	This work

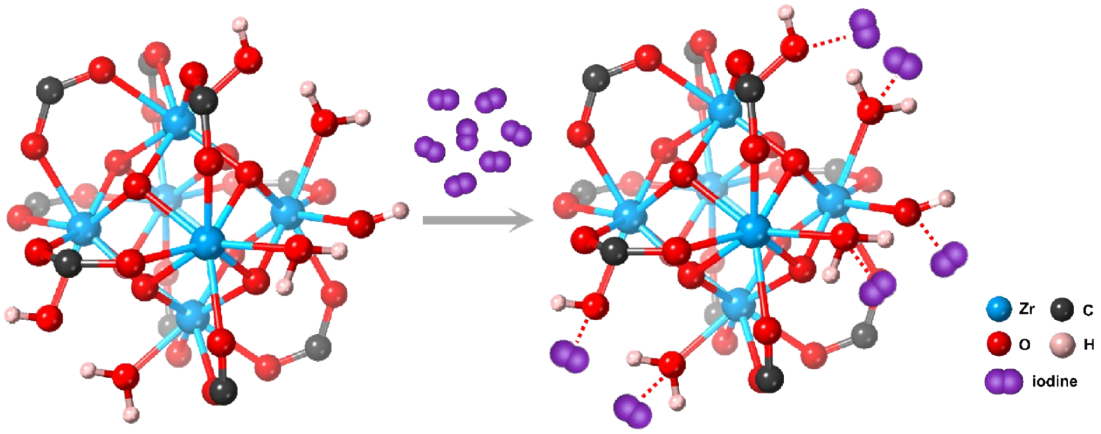

Fig. S8. Possible forms of interaction between zirconium cluster and iodine molecules.

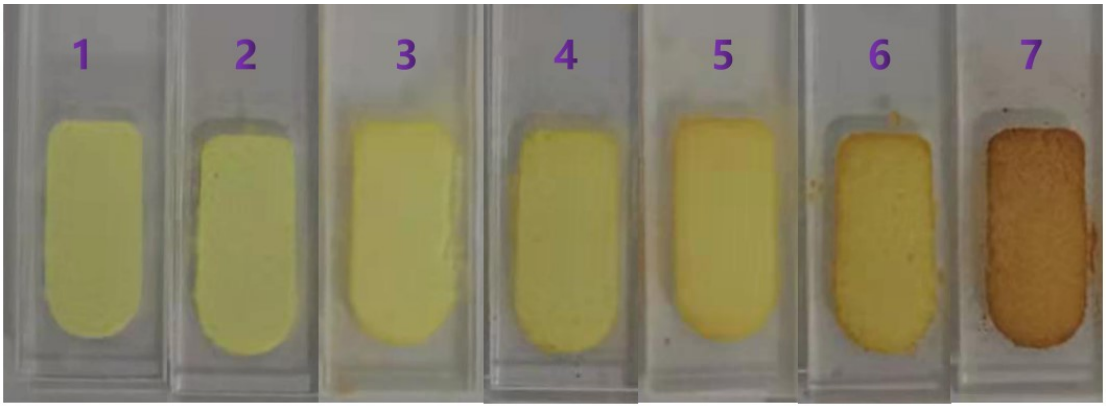

Fig. S9. Images showing **YTU-G-1** exposed to iodine vapor with different concentration (50, 100, 200, 300, 500, 700 and 1000 ppb) for 5 min.

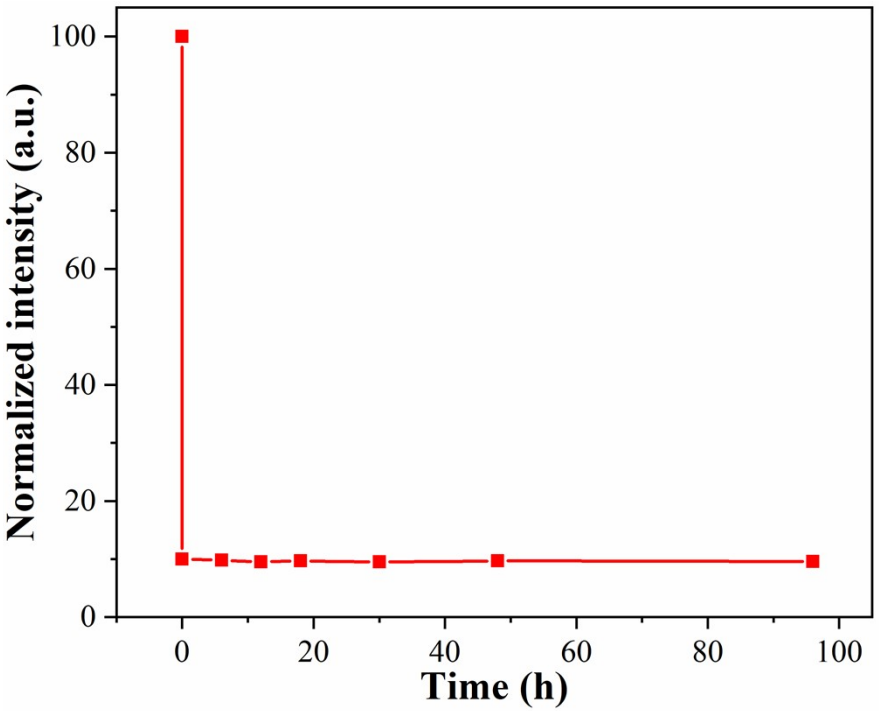

Fig. S10. The variation in luminescence intensity of **YTU-G-1** over time under ambient conditions after being quenched by iodine vapor.

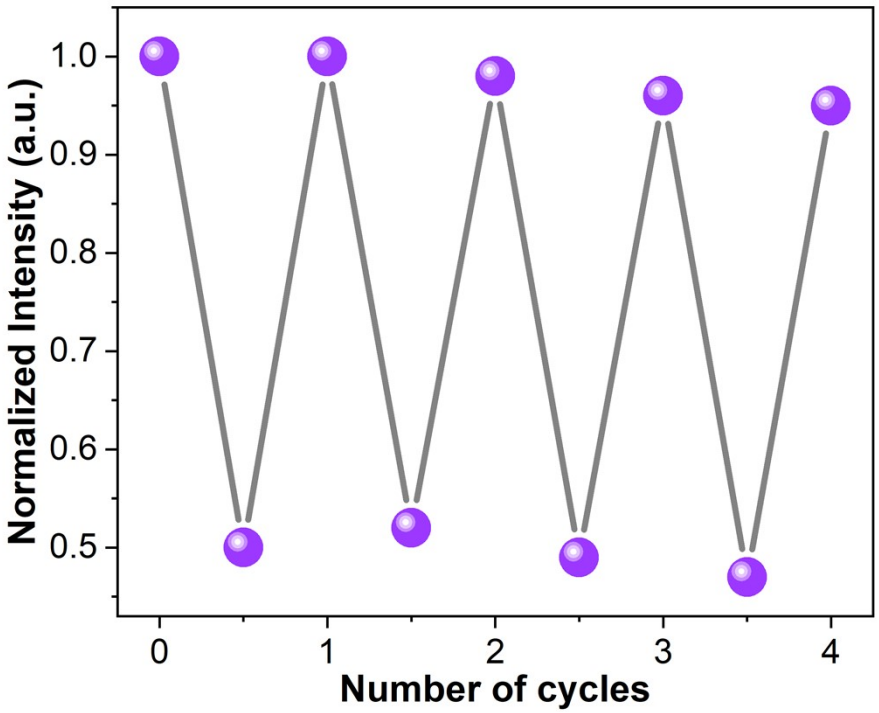

Fig. S11. The modulation of the photoluminescence intensity at 500 nm due to alternating exposure to 200 ppb iodine vapor for 5 min and 120 ^{o}C heating treatment for 12 h.

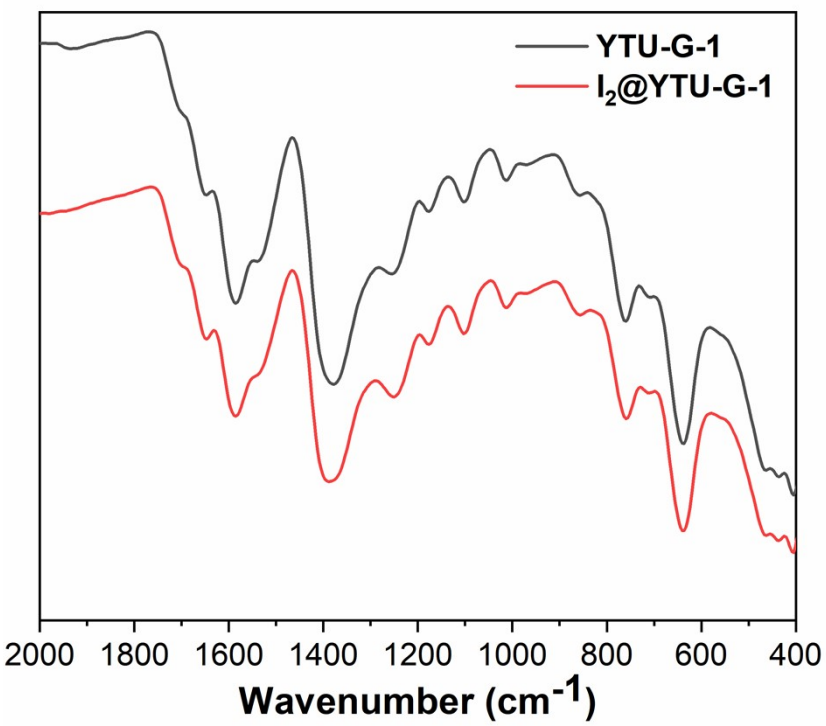

Fig. S12. FTIR spectra of the material before and after adsorption of iodine.

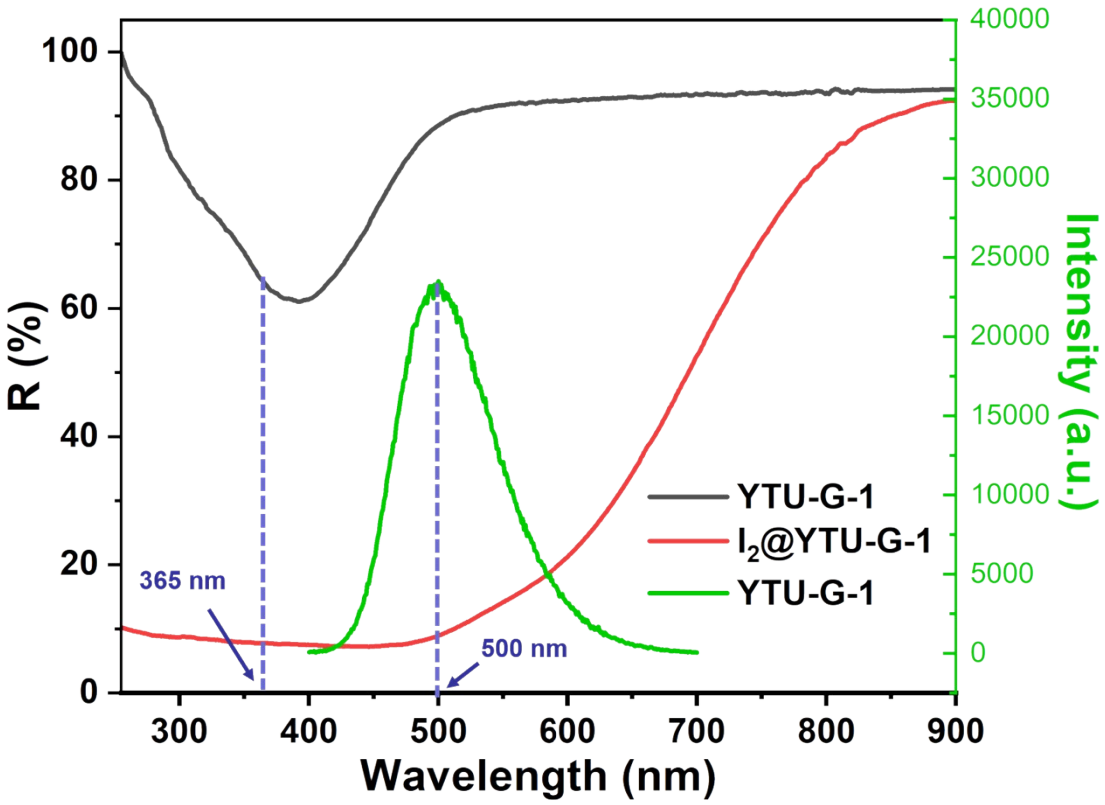

Fig. S13. Diffuse reflection spectra of the material before and after adsorption of iodine.

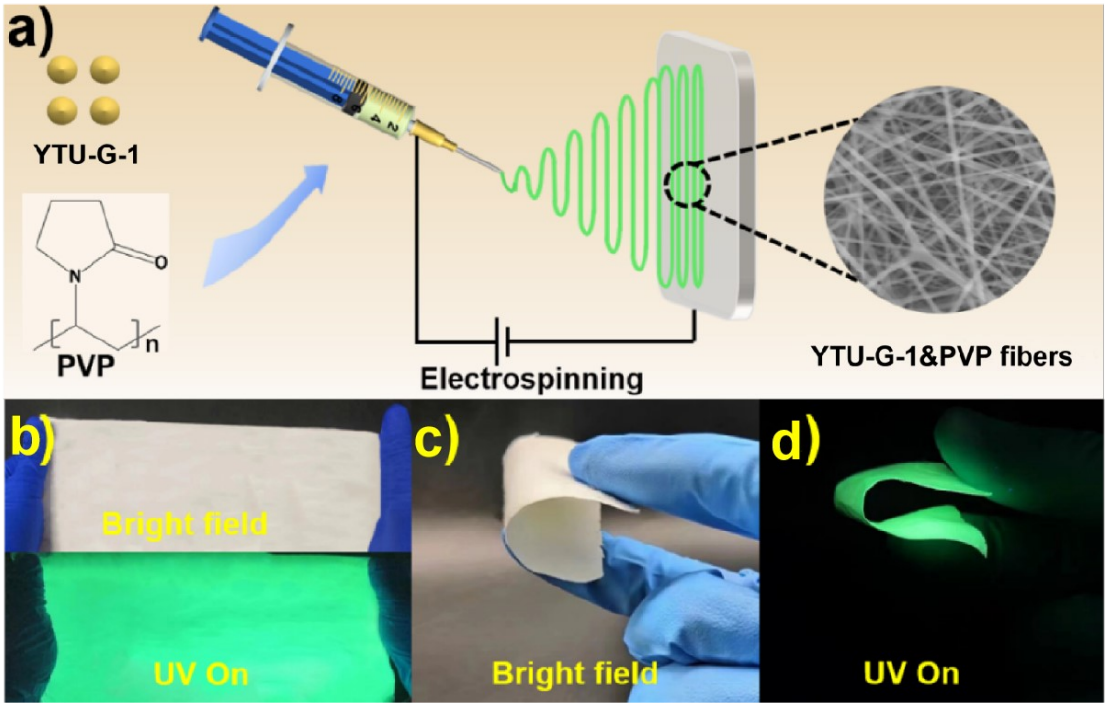

Fig. S14. (a) Schematic representation of the preparation of the composite **YTU-G-1**@PVP membrane. (b) Photograph of a **YTU-G-1**@PVP membrane prepared on clothing under UV light. (c-d) Photographs of a **YTU-G-1**@PVP membrane prepared on a rubber glove under sunlight and UV light.

Table S2. Summary of K_{SV} and LODs of materials for fluorescence sensing to iodine.

Sensor	Category	*K*sv (1/M)	LOD (mol/L)	Ref.
TBTZ	POPs	3.97×10^{3}	8.00×10^{-10}	Polym. Adv. Technol. 2023, 34, 1529-1539.
TPBTz	POPs	1.70×10^{5}	1.76×10^{-11}	J. Porous Mater. 2022, 29, 1565-1573.
PTThP-2	POPs	1.99×10^{3}	7.54×10^{-8}	J. Polym. Res. 2019, 26, 113-122.
PTThP-3	POPs	5.09×10^{3}	2.95×10^{-8}	J. Polym. Res. 2019, 26, 113-122.
TS-TAD	POPs	5.76×10^{3}	1.56×10^{-9}	Eur. Polym. J. 2019, 115, 37-44.
TS-TADP	POPs	5.59×10^{3}	8.05×10^{-11}	Eur. Polym. J. 2019, 115, 37-44.
TTPDP	POPs	2.02×10^{4}	2.25×10^{-12}	New J. Chem. 2020, 44, 2312-2320.
TDTPAP	POPs	4.65×10^{3}	3.25×10^{-10}	New J. Chem. 2020, 44, 2312-2320.
TTPATTh	CTFs	1.61×10^{4}	1.86×10^{-12}	Macromol. Mater. Eng. 2021, 306, 2100461.
TTPATCz	CTFs	3.10×10^{3}	3.87×10^{-11}	Macromol. Mater. Eng. 2021, 306, 2100461.
TIEPE-DABCO	XOFs	1.33×10^{5}	1.2×10^{-13}	Small 2023, 19, 2302902.
TDPDB	CTFs	5.83×10^{4}	2.57×10^{-12}	Polym. Adv. Technol. 2020, 31, 1388-1394.
TPG	POPs	2.01×10^{4}	5.98×10^{-10}	Macromol. Mater. Eng. 2021, 306, 2000711.
HCCPA	POPs	1.14×10^{4}	1.32×10^{-8}	Macromol. Mater. Eng. 2021, 306, 2000711.
TTPA	POPs	2.38×10^{4}	3.22×10^{-11}	Micropor. Mesopor. Mat. 2019, 273, 163-170.
TTTAT	POPs	1.53×10^{4}	2.98×10^{-12}	Micropor. Mesopor. Mat. 2019, 284, 468-475.
TTDAT	POPs	9.07×10^{4}	2.96×10^{-13}	Micropor. Mesopor. Mat. 2019, 284, 468-475.
TDPA	POPs	1.85×10^{4}	1.62×10^{-11}	J. Appl. Polym. Sci. 2020, 137, 49255.
TTPBTA	POPs	6.56×10^{4}	6.86×10^{-12}	J. Appl. Polym. Sci. 2020, 137, 49255.
TDPDB	POPs	5.83×10^{4}	2.57×10^{-12}	Polym. Adv. Technol. 2020, 31, 1388-1394.
TDP	POPs	6.10×10^{4}	3.14×10^{-13}	New J. Chem., 2020, 44, 2312-2320.
PCPP	POPs	1.40×10^{5}	2.46×10^{-12}	New J. Chem., 2020, 44, 2312-2320.
TDTPAPz	POPs	3.76×10^{3}	2.47×10^{-11}	Environ. Sci. Pollut. Res. 27, 20235-20245.
TTDPz	POPs	1.10×10^{3}	1.36×10^{-10}	Environ. Sci. Pollut. Res. 27, 20235-20245.
TBIM	POPs	1.16×10^{4}	1.29×10^{-10}	J. Mater. Chem. A, 2020, 8, 2820-2826.
PIM-1	PIMs	7.10×10^{4}	6.46×10^{-8}	Chem. Eng. J. 2022, 438, 135641.
IPIN-PVP	polymer	5.85×10^{3}	4.087×10^{-8}	Adv. Mater. 2024, 36, 2311990
YTU-G-1	MOGs	2.21×10^{6}	4.81×10^{-10}	This work